Identification of a new NEMO/TRAF6 interface affected in incontinentia pigmenti pathology

Jérémie Gautheron[1,†], Alessandra Pescatore[2,†], Francesca Fusco[2], Elio Esposito[2], Shoji Yamaoka[3], Fabrice Agou[4], Matilde Valeria Ursini[2,*,†] and Gilles Courtois[1,*,†]

[1]INSERM U781, Hôpital Necker-Enfants Malades and Université Paris-Descartes, 75015 Paris, France, [2]Institute of Genetics and Biophysics 'Adriano Buzzati-Traverso' (CNR), 80131 Naples, Italy, [3]Department of Molecular Virology, Tokyo Medical and Dental University, Tokyo 113-8519, Japan and [4]Unité de Biochimie Structurale et Cellulaire, Institut Pasteur, CNRS, URA 2185, 75015 Paris, France

NF-κB Essential MOdulator (NEMO) has been shown to play a critical role in NF-κB activation, as the regulatory subunit of IκB kinase. Upon cell stimulation, NEMO can be modified through phosphorylation, sumoylation or ubiquitination. In the latter case, not much is known regarding the exact function of this posttranslational modification. One of the E3 ligase responsible for K63-linked NEMO polyubiquitination is TRAF6, which participates in several signaling pathways controlling immunity, osteoclastogenesis, skin development and brain functions. We previously observed a potentially important interaction between NEMO and TRAF6. In this study, we defined in more detail the domains required for this interaction, uncovering a new binding site for TRAF6 located at the amino-terminus of NEMO and recognized by the coiled-coil domain of TRAF6. This site appears to work in concert with the previously identified NEMO ubiquitin-binding domain which binds polyubiquitinated chains, suggesting a dual mode of TRAF6 recognition. We also showed that E57K mutation of NEMO found in a mild form of the genetic disease incontinentia pigmenti, resulted in impaired TRAF6 binding and IL-1β signaling. In contrast, activation of NF-κB by TNF-α was not affected. These data demonstrate that NEMO/TRAF6 interaction has physiological relevance and might represent a new target for therapeutic purposes.

INTRODUCTION

The NF-κB family of transcription factors represents a collection of dimeric proteins formed by associations between p50/p105, p52/p100, c-rel, relA and relB. NF-κB has been shown to play key roles in numerous physiological processes such as immunity, inflammation, cell growth and apoptosis (1,2). In resting cells, NF-κB is retained in the cytoplasm, through interaction with IκB molecules. Following stimulation, IκBs are phosphorylated, inducing recognition by the βTRCP complex, ubiquitination and degradation by the 26S proteasome. As a consequence, free NF-κB translocates into the nucleus and activates its target genes.

Phosphorylation of IκB, which is critical for NF-κB activation, is carried out by a kinase complex, IKK (IκB

kinase), composed of three major subunits: IKK1/IKKα, IKK2/IKKβ and NEMO (NF-κB Essential MOdulator)/IKKγ (3). IKK1 and IKK2 are two structurally related kinases, whereas NEMO has no catalytic activity, behaving as a regulatory subunit. IKK can be activated by a broad range of stimuli, among them pro-inflammatory cytokines such as TNF-α and IL-1β, bacterial products such as LPS and LPA, or various forms of stress (4).

Deregulation of all these processes has been reported to occur in patients suffering from the X-linked genetic disease incontinentia pigmenti (IP) (5) which is caused by mutation of the gene *IKBKG* encoding NEMO (6,7). The main feature of the disease is a dermatosis which usually starts within 2 weeks after birth and evolves along a complicated sequence of events, featuring inflammation and hyper-proliferation of

keratinocytes, before regressing. Its exact cellular and molecular basis remains incompletely understood (8). In addition, a large fraction of IP patients exhibit ocular and odontological problems and a small percentage of them suffer from central nervous system abnormalities which can result in severe epilepsy and mental retardation. In most IP patients (approximately 70–80%), an identical DNA rearrangement occurs and produces a severe truncation of the NEMO protein. More interestingly, rare missense mutations of *NEMO* causing IP have been described over the years (9). Their detailed analysis at the molecular level represents an interesting opportunity to get more insights into the mechanisms leading to IKK activation. In addition, understanding how they are distinguishable from *NEMO* mutations generating another genetic disease characterized by immunodeficiency and impaired development of skin adnexa, EDA-ID (7), should provide valuable information about the regulation of NF-κB function *in vivo*.

The IKK activation process is under intense investigation but remains incompletely understood. It was originally shown by Chen's lab to depend on ubiquitination processes which are different from the ones leading to protein degradation, like in the case of IκBα (10). Ubiquitination consists in the covalent addition of ubiquitin, a 76 amino acid peptide, to substrates (11). It requires a sequence of reactions involving three main components. First, an ubiquitin activating enzyme (E1) catalyses the formation of a thioester bond between the C-terminus of ubiquitin and its active cysteine. Then, ubiquitin is transferred to a conjugating enzyme (E2), forming an E2-ubiquitin thioester. Finally, ubiquitin is covalently attached to substrates through formation of isopeptide bonds between the C-terminus of ubiquitin and the ε-amino group of lysines. The enzymes responsible for this final step, the ubiquitin ligases (E3), are the ones that provide target specificity by directly interacting with the substrates that are prone to ubiquitination (12). Depending on the E2/E3 machinery assembled, mono- or polyubiquitination of proteins can be achieved. Polyubiquitination is made possible by the presence of seven lysines in ubiquitin. When K48-linked polyubiquitinated chains are synthesized, this results in recognition and degradation by the proteasome. In contrast, when K63-linked chains are added to proteins, no degradation is observed but their function is modified by various mechanisms. For instance, ubiquitination can provide a platform for recruiting partners, an event which requires the presence in the partner of protein domains [ubiquitin interacting motifs (UIMs)] which specifically recognize Ub chains (13).

In the case of NF-κB signaling, K63-linked ubiquitination has been observed to modify several distinct molecules participating in IKK activation (14). In addition, some components of signaling pathways leading to IKK/NF-κB activation exhibit ubiquitin-binding properties. This provides a complex framework of protein/protein interactions which are fine-tuned by enzymes with deubiquitinating activity such as A20 and CYLD (15). In several instances, this framework has been elucidated to some extent. When cells are exposed to TNF, cIAP1/2 and TRAF2 are the E3 ligases participating in RIP ubiquitination and recruitment of the TAK complex through TAB2/3 subunits, which exhibit affinity for polyubiquitinated chains, and IKK, through NEMO which is also an ubiquitin-binding protein. This results in IKK1/2 phosphorylation by TAK1 and subsequent NF-κB activation (16). In the case of IL-1 and LPS signaling, which require members of the IL-1/TLR family of receptors, a complex set of events downstream the receptors results in IRAK-1 binding to E3 ligase TRAF6. At this level, TRAF6 and IRAK-1 are polyubiquitinated and recruit TAK and IKK (17). In this specific pathway, it has been proposed that NEMO is ubiquitinated by TRAF6, in addition to participating in IKK recruitment through its affinity for Ub chains (18). Nevertheless, the putative role of this modification remains unclear. We have previously identified the lysine residues of NEMO which are targeted by TRAF6, exploiting the identification of a new NEMO mutation causing IP, and detected an interaction between these two molecules (19). In this paper, we report the characterization of the domains participating in NEMO/TRAF6 interaction and provide genetic and molecular evidence supporting their role in NF-κB activation.

RESULTS

Interaction between TRAF6 and the amino-terminus of NEMO

Whereas A323P mutation in human(h) NEMO reduced binding to TRAF6 and almost completely abolished ubiquitination of surrounding lysines (19), an equivalent mutation in mouse(m) NEMO (V316P) bound TRAF6 as well as wild-type (wt) mNEMO, although exhibiting reduced ubiquitination (Fig.1A, compare lanes 11–12 with lanes 5–6). This confirmed the effect of mutating this region of NEMO on its ubiquitination by TRAF6 but also suggested the presence of an additional domain of interaction between NEMO and TRAF6.

To localize this domain, we used several versions of mNEMO. Carboxy-terminal truncations (ΔC385, ΔC343 and ΔC299) did not affect TRAF6 binding (Fig.1B). Similarly, several internal deletions of mNEMO (Δ113–168, Δ201–255 and Δ250–311) were still able to interact with TRAF6 (Fig.1C). This suggested that the amino (N)-terminal part of the protein may be involved in TRAF6 binding. The effect of several small internal deletions located at the N-terminus of NEMO (20) was therefore investigated. Removing amino acids 47–56 (Δ47–56) reduced TRAF6 binding to some extent, whereas removing amino acids 57–69 (Δ57–69) was very deleterious (Fig.1D, compare lanes 7–8 and 5–6, respectively, with lanes 1–2). In contrast, removing amino acids 70–79 (Δ70–79) appeared without any effect (Fig. 1D, lanes 3–4) although known as affecting IKK2 binding (20). Importantly, interaction of Δ57–69 mutant with IKK2, which is supposed to recognize a sequence from approximately amino acids 80–100, remained unaffected as previously reported (20, data not shown). This indicated that the lack of interaction between Δ57–69 and TRAF6 was not caused by an extended desorganization of the NEMO N-terminus. Instead, a specific sequence recognizing TRAF6, distinct from the IKK2 binding site, appeared to be present in this part of the molecule.
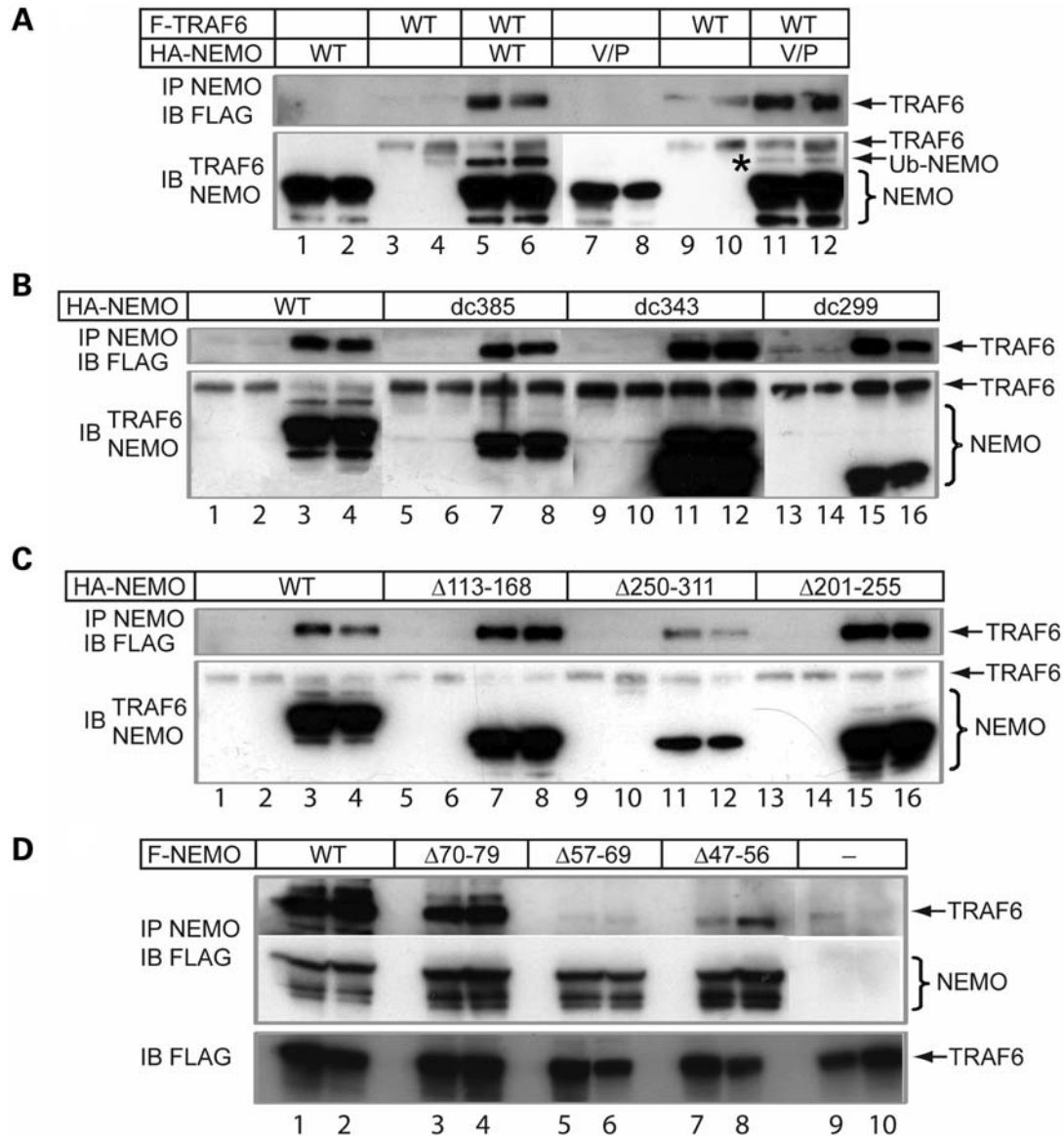
Figure 1. Identification of a new TRAF6 binding domain located at the N-terminus of NEMO. HEK 293T cells were transiently co-transfected with various forms of NEMO and Flag-TRAF6. Whole-cell extracts were prepared 24 h later, immunoprecipitated with anti-NEMO and analysed, after western blotting, with anti-Flag. The effect of V/P mutation (**A**), C-terminal truncations (**B**) or internal deletions (**C** and **D**) of NEMO on TRAF6 binding is shown in the upper panels. The expression of the various proteins is shown in the lower panels. IP, immunoprecipitation; IB, immunoblotting. The asterisk in (A) indicates a lack of ubiquitinated for V/P mutation.

E57K, a mutation of NEMO causing incontinentia pigmenti, is defective in TRAF6 binding

Several missense mutations (E57K, D113N and R123W) and a short three nucleotide deletion of NEMO (ΔK90), which have been shown to cause incontinentia pigmenti (21), are located within the first 150 amino acids of the protein but, in the case of the three mutations, no associated molecular defects had been reported so far. We therefore examined their impact on NEMO/TRAF6 interaction. Two of them, E57K and ΔK90, exhibited reduced interaction with TRAF6 (Fig. 2A, lanes 5–6 and 7–8, respectively), whereas D113N and R123W behaved like wt NEMO. In contrast to mutation ΔK90, which has been shown to affect binding of NEMO to

IKK catalytic subunits (21), maybe because of a path change in a region with helical structure (22), mutation E57K did not affect binding of NEMO to IKK2 (Fig. 2B). This confirmed distinct sequence requirements for TRAF6 and IKK binding, as already suggested by the analysis of Δ57–69 deletion (see above).

As shown in the study of Rushe *et al.* (22), residue E57 is able to establish *in trans* a contact with residue R62, through an electrostatic bond involving the carboxyl group of E57 and the guanidium group of R62 (Fig. 3A). A change from Glu to Lys may therefore affect this interaction, by introducing a repulsive charge and distort to some extent the short helical domain (αh1) located nearby the IKK binding domain and reported to participate in NEMO
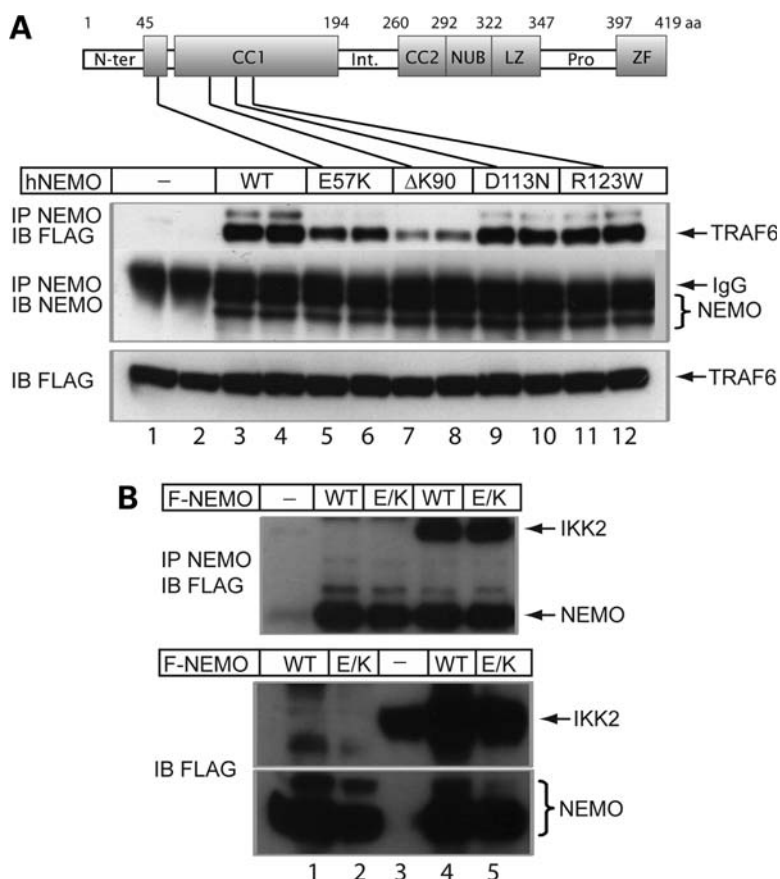
Figure 2. Defective binding of TRAF6 to IP-associated E57K mutant. (**A**) HEK 293T cells were transiently transfected with Flag-TRAF6 and various Incontinentia Pigmenti-related missense mutations of hNEMO whose location within the NEMO protein is indicated. Cell lysates immunoprecipitated with anti-NEMO were probed with anti-Flag and anti-NEMO antibodies after immunoblotting (upper panel). Expression of TRAF6 in whole-cell lysates was verified with anti-Flag antibody (lower panel). CC, coiled coil 1; Int., intermediate domain; NUB, NEMO ubiquitin-binding domain; LZ, leucine zipper; ZF, zinc finger; IgG, immunoglobulin G. (**B**) 293T cells were co-transfected with wt hNEMO or E57K (E/K) NEMO and Flag-IKK2, immunoprecipitated with anti-NEMO and analysed using anti-Flag (upper panel). The expression of NEMO and IKK2 was verified using anti-Flag and anti-NEMO (lower panel).

dimerization (20), indirectly resulting in impaired TRAF6 binding. Alternatively, a change in amino acid or charge at E57 may directly affect NEMO recognition by TRAF6. To distinguish between these two possibilities, we mutated R62 by also introducing a charge change (R62E). As shown in Figure 3B, binding of TRAF6 to R62E NEMO was not perturbed (Compare lanes 5–6 with 3–4), suggesting that E57 residue establishes a direct contact with TRAF6.

E57K mutant is impaired in IL-1 and TRAF6 signaling

Despite repeated attempts, we were unable to detect a reproducible reduction of NF-κB activation in response to IL-1 or LPS when NEMO (-) 1.3E2 cells (23) or NEMO (-) MEFs (24) were transiently complemented with E57K NEMO (21, data not shown). Because this mutation has been associated with a mild form of IP, we generated stable MEFs cells expressing wt or E57K NEMO at physiological levels in order to more faithfully reflect its putative effect on NF-κB signaling. As shown in Figure 4A, pools of MEFs expressing at identical level wt or E57K NEMO were obtained after retroviral transduction (compare lanes 2 and 3). Importantly, this level of expression was similar to the endogenous level of NEMO in

wt MEFs (lane 1) and E57K mutation did not affect integration of NEMO into IKK after transfecting the cells with IKK2 (Fig. 4B, compare lane 2 with 3).

Upon IL-1β exposure, NF-κB transcriptional activation in E57K-expressing cells appeared significantly reduced when compared with wt NEMO-expressing cells (approximately 54 ± 13% of wt) (Fig. 4C). In accordance with what is presented above, regarding a defective interaction between E57K NEMO and TRAF6, activation of NF-κB by TRAF6 overexpression was also strongly reduced in E57K cells (approximately 46 ± 5% of wt). In striking contrast, mutation E57K did not affect NF-κB transcriptional activation when TNF-α was used instead of IL-1. This demonstrated that IP-related E57K mutation was specifically associated with impaired NF-κB stimulation in response to IL-1, most likely due to an impaired interaction with TRAF6.

Dual mode of recognition between NEMO and TRAF6

To confirm the observations reported above concerning a TRAF6 binding domain located at the N-terminus of NEMO, we analyzed the interaction between TRAF6 and ΔN97 mNEMO, which lacks the whole N-terminal sequence
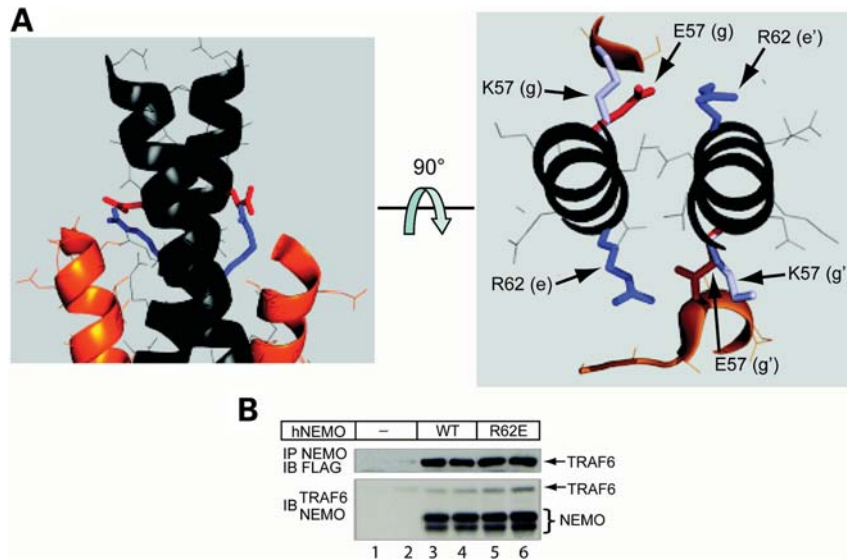
Figure 3. Structural consequences of E57K mutation. (**A**) The effect of introducing a Lys residue (light blue) at position 57 is shown. The broken lines between Glu57 (red) and Arg62 (dark blue) indicates a salt bridge which is destroyed by E57K mutation. Positions along the α-helices are also indicated (e, e′, g, g′). (**B**) Effect of R62E mutation on TRAF6 binding. The experiment was carried out as described in Fig. 2A.

of NEMO including the IKK binding site. To our surprise, this truncation was still able to co-immunoprecipitate TRAF6 (Fig. 5A, lanes 9–10). We therefore considered the possibility that, in the context of a full-length mouse NEMO molecule, binding of TRAF6 may predominantly involve the N-terminus of NEMO, whereas deletion of this N-terminus may somehow unmask the second site of interaction originally observed when studying human NEMO (19). Importantly, this second site involves residue A323 (V316 in the mouse), which has been shown to be located very close to the NEMO ubiquitin-binding (NUB) domain of NEMO, responsible for polyubiquitin binding, and to affect the interaction between NEMO and ubiquitin when mutated to Pro (25,26). The possibility that it was involved in binding to ubiquitinated TRAF6 through ubiquitin moieties rather than directly to TRAF6 was therefore investigated.

We first confirmed, using a GST pull-down assay, that hNEMO preferentially interacted with ubiquitinated TRAF6 (Fig. 5B, lanes 5–6) and that mutating residue Ala323 abolished this interaction (lanes 13–14). Then, we demonstrated that ΔN97 mNEMO exhibited affinity for wt TRAF6 after co-transfection in HEK293T cells, but interacted very weakly with a mutant of TRAF6 (C70A TRAF6) possessing a defective ring finger and therefore unable to auto-ubiquitinate (Fig. 5A, compare lanes 17–18 with 13–14). Furthermore, introducing a V316P mutation into ΔN97 also reduced the interaction with TRAF6 (Fig. 6A, compare lanes 9–10 with 7–8). This was in striking contrast to what had been observed with wt mNEMO (Fig. 1). Finally, we were able to show that interaction between ΔN97 mNEMO and TRAF6 was very sensitive to co-expression of CYLD, a deubiquitinase binding to the C-terminus of NEMO and displaying affinity for K63-linked polyubiquitin chains (27), whereas interaction between wt mNEMO and TRAF6 was almost insensitive (Fig. 6B, compare lanes 15–16 with 7–8). The sum of these observations suggests a dual mode of

recognition between NEMO and TRAF6 in our cell system. On one hand, TRAF6 may directly contact the N-terminus of NEMO at a site distinct from, but close to, the one involved in IKK binding and, on the other hand, polyubiquitin chains of TRAF6 may interact with the NUB domain.

The coiled-coil domain of TRAF6 interacts with NEMO

Several truncated forms of TRAF6 were examined for their ability to interact with NEMO (Fig. 7). Removal of the first 108 or 297 amino acids of TRAF6 (ΔN108 and ΔN297), which eliminated the ring finger only or both the ring finger and the five zinc fingers did not affect binding of TRAF6 to NEMO (Fig. 7B, lanes 11–12 and Fig. 7C, lanes 5–6). In contrast, the interaction was lost when deleting N-terminal portions of the TRAFN domain such as in ΔN319 and ΔN330 (Fig. 7C, lanes 7–8 and 9–10, respectively). Conversely, deleting the TRAF-C domain of TRAF6 did not affect binding of TRAF6 to NEMO (Fig. 7B, lanes 11–12), but eliminating N-terminal portions of the TRAFN domain, such as in ΔC325 and ΔC308, impaired NEMO binding (Fig. 7D, lanes 5–6 and 7–8). This suggested that the TRAFN domain of TRAF6, which has the structure of a coiled coil (CC), may be responsible for TRAF6 interaction with the N-terminus of NEMO. To support this hypothesis, an internal deletion of TRAF6 lacking residues 307–332, which are the most conserved in the coiled coil of TRAF6 proteins, was engineered. The mutant protein (ΔCC-TRAF6) exhibited a strong defect in NEMO binding (Fig. 8A, compare lanes 7–8 with 5–6). In contrast, ΔCC-TRAF6 was still able to properly interact with another partner, IRAK1, which recognizes TRAF6 through its TRAF-C domain (Fig. 8B).

To exclude the possibility that the interaction between the coiled coil of TRAF6 and the N-terminus of NEMO was caused by some non-specific interaction occurring between two amphipatic helices, we studied the binding of NEMO to
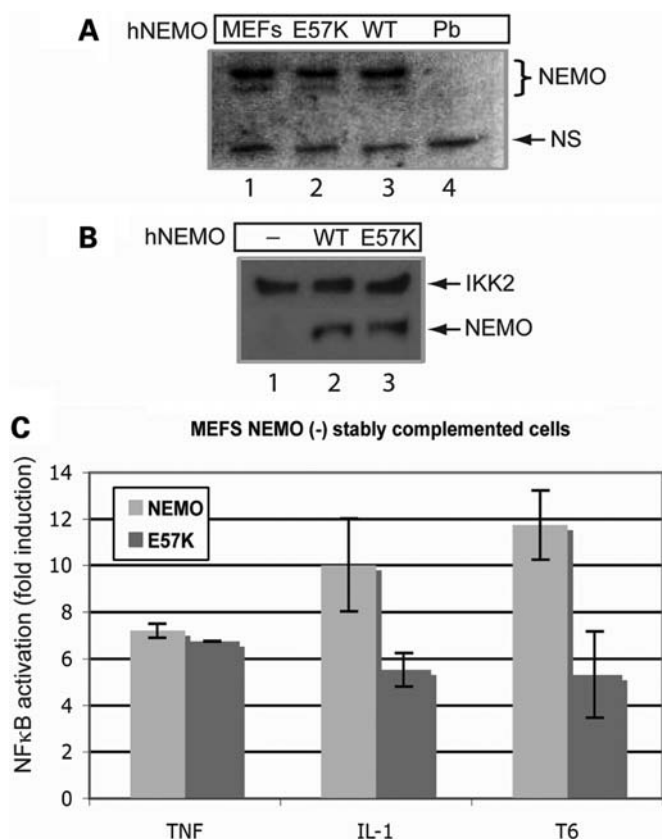
Figure 4. Functional analysis of E57K mutation. (**A**) Western blot analysis of NEMO in wt MEFs and NEMO (-) MEFs stably complemented with empty pBabe vector (pB), pBabe expressing wt NEMO or expressing mutant E57K. A non-specific band (n.s.) revealed by the antibody demonstrates equal loading between the samples. (**B**) E57K mutant interacts normally with IKK2. MEF clones were transfected with Flag-IKK2, then IKK2 was IP with anti-Flag and analyzed for associated NEMO (**C**) NF-κB transcriptional activation. Complemented MEFs were stimulated with TNF-α, IL-1β or TRAF6 and NF-κB activation was measured using a luciferase assay as described in Materials and Methods. Fold activation is shown. Error bars represent variation ranges of duplicate experiments.

TRAF2, another member of the TRAF family that also contains a coiled-coil domain located upstream of its TRAF-C domain. No interaction between TRAF2 and NEMO was observed (Fig. 8C).

The coiled-coil domain of TRAF6, which interacts with NEMO, is required for NF-κB activation

In order to confirm that binding of TRAF6 to NEMO through the coiled-coil domain of TRAF6 was required for NF-κB activation, we transfected HEK 293T cells with wt TRAF6, C70A TRAF6, ΔC351-TRAF6, ΔC325-TRAF6, ΔC308-TRAF6 or ΔCC-TRAF6 and looked for NF-κB activation using an Igκ-luc reporter plasmid. As shown in Figure 9, activation of NF-κB by TRAF6 was completely dependent upon its E3 ligase activity since C70A TRAF6 was totally inactive. Moreover, ΔC351-TRAF6 was still able to activate NF-κB at the same level as wt TRAF6, despite its inability to interact with IRAK-1 (data not shown). In contrast, ΔC325-TRAF6 and Δ308-TRAF6, which were expressed at the same level

as wt TRAF6 (data not shown), appeared much less potent. Finally, ΔCC-TRAF6 exhibited a quite reduced activity, between 25 and 35% of the activity of TRAF6 wt. This indicates that the coiled coil of TRAF6, which interacts with NEMO, is required for NF-κB activation.

DISCUSSION

In order to get more insights into the NF-κB activation process, we have initiated a molecular analysis of NEMO missense mutations causing the genetic disease incontinentia pigmenti. Such analysis is expected to uncover new features of the protein and to allow a better understanding of its role in IKK activation. In addition, this work should provide useful information regarding the molecular basis of the disease and the specific pathways that are deregulated. Here, we confirmed that NEMO and TRAF6 interact with each other and demonstrated that the novel identified interface can be affected by pathology-associated mutations.

The NF-κB activation process is largely dependent upon ubiquitination processes which either result in protein degradation or regulate the function of several molecules directly participating in IKK stimulation. These events involve specific E3 ligases and, among them, various members of the TRAF family of proteins. In particular, TRAF6 has been shown to play key roles in NF-κB-dependent signaling pathways that control immunity, osteoclasteogenesis, skin development and brain function. It therefore represents an attractive target for inhibiting NF-κB activation when this activation is deregulated, such as in inflammation, cancer or autoimmunity.

How TRAF6 participates in IKK activation remains unclear. It has been originally proposed that cell stimulation induces its autoubiquitination, helping recruiting the TAK complex through TAB2- and TAB3-associated subunits which contain NZF domains (28). Nevertheless, this model has been recently challenged by the demonstration that a TRAF6 protein mutated in all of its lysines was still able to activate NF-κB (29). Since the E3 ligase activity of TRAF6 is unambiguously required for NF-κB activation (30, Fig. 9), this would mean that this protein acts by ubiquitinating a partner instead of itself. Among the putative candidates are IRAK-1 and NEMO. Both of them have been shown to interact with TRAF6 but the role of these interactions is still uncertain. For instance, IRAK-1 has been shown to be ubiquitinated upon IL-1 stimulation and Ashwell's group has proposed that the E3 ligase involved was TRAF6 (31). In contrast, Cohen's group has reported that Pellino, instead of TRAF6, was the E3 for IRAK-1 (32). The consequence of this IRAK modification would be the recruitment of IKK through NEMO, as shown by the inability NEMO mutated in its NUB to activate NF-κB.

We and others have shown, using overexpression or *in vitro* assays, that TRAF6 was also able to ubiquitinate NEMO (19,33), but the exact relationship between this modification and IKK activation remains elusive. To further complicate the picture, it has been proposed that NEMO may also be modified by linear polyubiquitination in pathways involving TRAF6, such as the IL-1 pathway. In this case, the E3 modifying NEMO appears to be a dimeric protein termed LUBAC
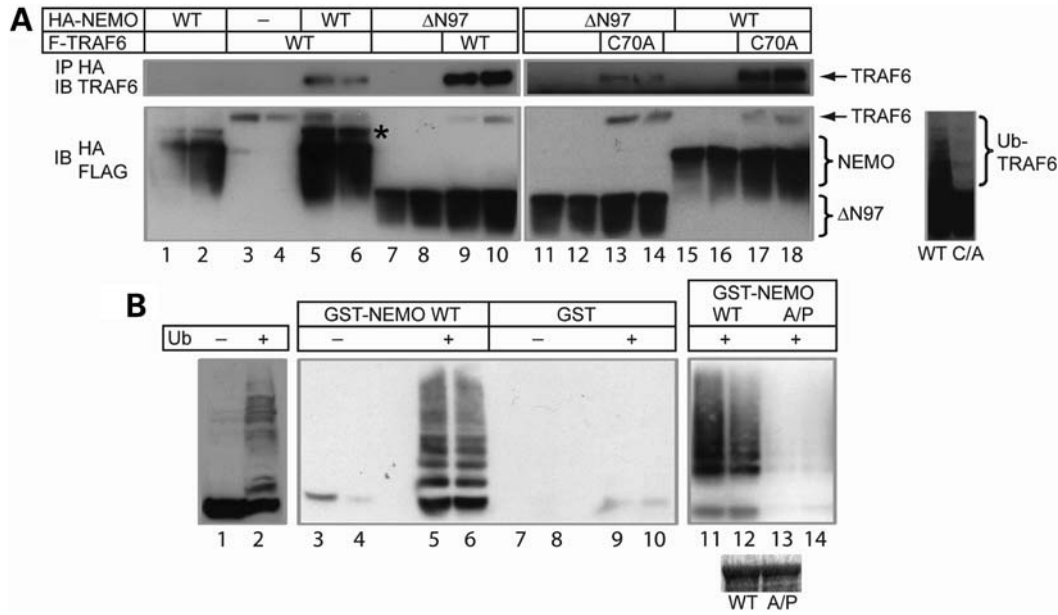
Figure 5. Interaction between NEMO and ubiquitinated TRAF6. (**A**) Extracts from HEK 293T cells transiently transfected with wt HA-NEMO or ΔN97 alone or in combination with Flag-TRAF6 or Flag-C70A TRAF6, were analyzed with anti-TRAF6 after immunoprecipitation with anti-HA. The asterisk indicates ubiquitination of wt NEMO which does not occur anymore following elimination of the first 97 amino acids. (**B**) GST, GST-NEMO or GST-A/P NEMO bound to gluthation-Sepharose beads, prepared as described in Materials and Methods, were incubated with lysates derived from cells previously transfected with Flag-TRAF6 alone or with HA-Ub (Ub). Bound TRAF6 was released from the beads and analyzed after western blotting with anti-TRAF6. The lower panel on the right represents a Coomassie staining of GST-NEMO and GST-A/P NEMO beads.
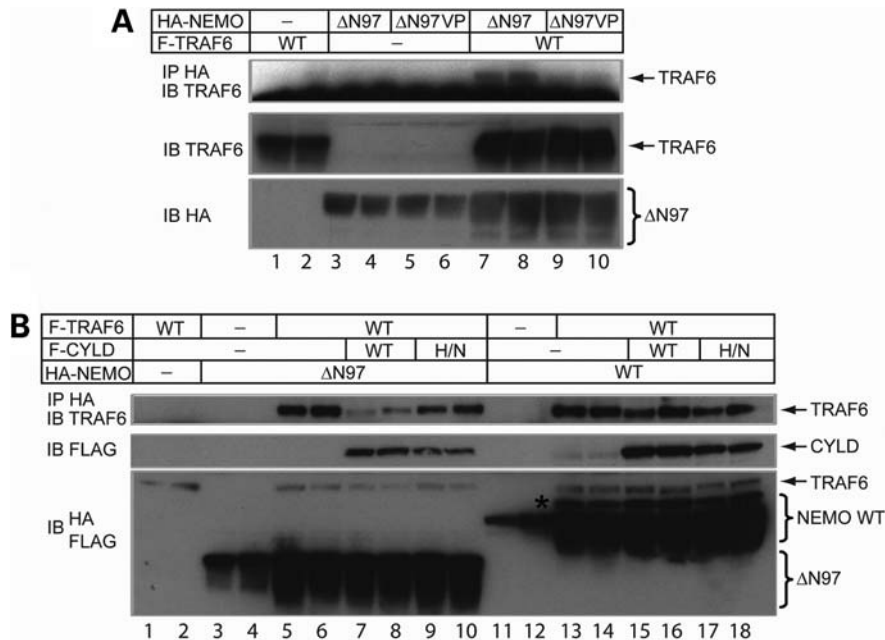

Figure 6. Binding of NEMO to TRAF6 through the NUB domain. (**A**) Extracts from HEK 293T cells transiently transfected with ΔN97 or V316P ΔN97 alone or in combination with Flag-TRAF6 were analyzed with anti-TRAF6 after immunoprecipitation with anti-HA. The asterisk indicates ubiquitination of wt NEMO which does not occur anymore following elimination of the first 97 amino acids. (**B**) Extracts from HEK 293T cells transiently transfected with wt NEMO or ΔN97 and Flag-TRAF6 and the effect of also co-transfecting wt or catalytically inactive (H/N) Flag-CYLD on NEMO/TRAF6 interaction was also checked after immunoprecipitation with HA and analysis with anti-TRAF6.

which is composed of two distinct E3 proteins, HOIL-1L and HOIP (34).

Here, we demonstrate that the binding of TRAF6 to NEMO involves two distinct domains of the NEMO protein (Fig. 10).

The first one had been previously identified during our molecular characterization of the IP-associated A323P mutation (19). We believe that it acts through recognition of ubiquitinated TRAF6 and coincides with the NUB domain, based on
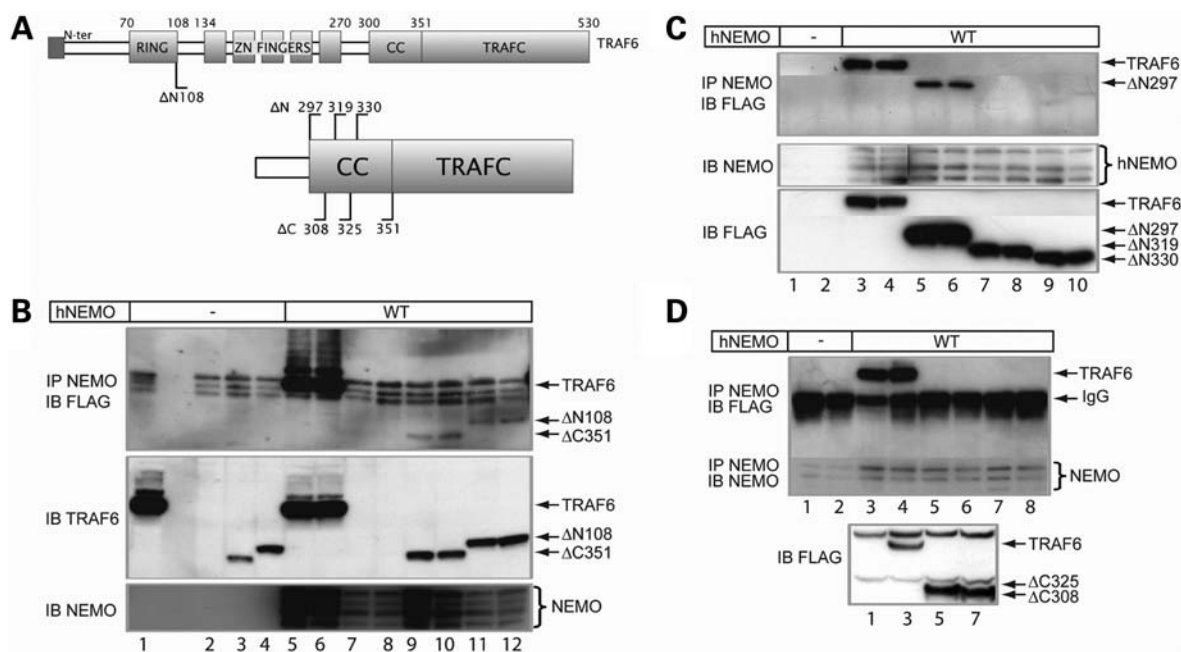
Figure 7. The coiled-coil domain of TRAF6 interacts with NEMO. (**A**) Schematic diagram of TRAF6 representing the RING, zinc (ZN) finger, coiled-coil (CC) and TRAF-C domains. The different deletions analyzed are indicated. (**B**) HEK 293T cells were transiently transfected with expression vectors encoding hNEMO alone or with expression vectors encoding Flag-TRAF6, Flag-TRAF6 ΔC351 or Flag-TRAF6 ΔN108. Twenty four hours post-transfection whole-cell extracts were prepared and immunoprecipitated using anti-NEMO. The samples were analyzed after immunoblotting with anti-Flag (upper panel). Expression of the various expressed proteins is also shown (lower panels) (**C** and **D**). A similar co-immunoprecipitation assay using hNEMO and various amino- or carboxy-terminal deletion of TRAF6.

the following observations: (i) it involves a region of NEMO located near the NUB domain; (ii) it requires residue A323 (V316 in the mouse), an amino acid important for ubiquitin recognition (25,26); (iii) it is sensitive to the deubiquitinase activity of CYLD, as shown using ΔN97. At this stage, we can not formally exclude that this domain also recognizes *in vivo* ubiquitin moieties of a partner of TRAF6, such as IRAK1, instead of ubiquitinated TRAF6 itself (see above). The second domain, which is novel, is located at the N-terminus of the protein and most probably establishes a direct contact with TRAF6, not sensitive to CYLD. Worth noting, binding of TRAF6 to this domain appears absolutely required for NEMO ubiquitination, since ΔN97 is not modified upon co-transfection with TRAF6 despite its conserved ability to pull-down ubiquitinated TRAF6.

The N-terminal part of the NEMO molecule has been reported to bind IKK1 and IKK2 but other regulators of IKK, such as CIKS/Act1, ATM, PIASy and NESCA interact there as well (35–38). For some of them, it remains nevertheless unclear whether this interaction is physiologically relevant. In our case, impaired interaction of TRAF6 with this site results in defective NF-κB activation by IL-1, as observed with IP-related E57K mutation.

Recent studies have demonstrated that the N-terminal part of NEMO is composed of short helices, which not only provide interfaces for heterotypic interaction with IKK1/IKK2 but also allow dimerization of NEMO. For instance, a structural analysis of the NEMO/IKK interaction domain has identified several critical residues participating either in recognition by IKKs or NEMO dimerization (22). Moreover,

Marienfeld *et al*. (20) have functionally dissected the N-terminal part of NEMO and demonstrated that it can be divided into two distinct subdomains. Interestingly, Δ57–69 mutant which appears perturbed in N-terminus dimerization is still able to interact with IKK1 and IKK2, suggesting that it performs another function than structuring the IKK binding site.

On the TRAF6 side, our study has revealed a new putative function of the TRAF6 coiled coil as a NEMO binding interface. Until now, the role of this domain was quite unclear besides its possible participation in TRAF6 oligomerization. This contrasts with the well-known functions of the ring finger and TRAF-C domains. Yang *et al*. (39) have proposed that the coiled coil of TRAF6 was required for TRAF6 auto-ubiquitination and NF-κB activation through its binding to Ubc13. Nevertheless, the Ubc13 binding domain is supposed to be the ring finger, specifically dedicated to the interaction with the E2 conjugating enzymes (40). We show here that the TRAF6 coiled coil may perform an additional/alternative function, NEMO binding, that would explain its role in NF-κB activation.

What might be the role of the NEMO/TRAF6 interaction we have characterized? Ubiquitination of NEMO has been reported in several instances. Therefore, TRAF6 may represent a *bona fide* NEMO E3 ligase. Nevertheless, TRAF6 usually works in concert with Uev1a/Ubc13 to synthesize K63-linked polyubiquitin chains and there is a controversy regarding the kind of chains that modify NEMO upon stimulation, including IL-1β stimulation. Indeed, it has been proposed that NEMO may be modified by K63-linked chains
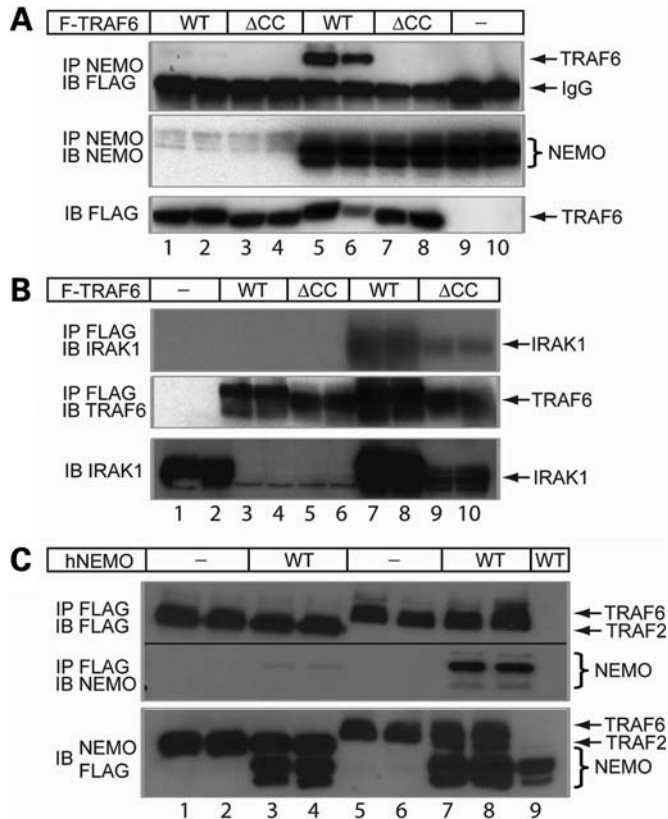
Figure 8. The coiled-coil domain of TRAF6 is specifically recognized by NEMO. (**A**) Defective interaction of ΔCC-TRAF6 with NEMO. The analysis was carried out as described in Fig. 7. (**B**) Interaction of wt TRAF6 and ΔCC-TRAF6 with IRAK1. HEK 293T cells were transfected with expression vectors encoding TRAF6 and IRAK1. Immunoprecipitations were performed using anti-Flag and the samples were analyzed after immunoblotting with anti-IRAK1. (**C**) TRAF2 does not interact with NEMO. HEK 293T cells were transfected with expression vectors encoding NEMO, Flag-TRAF6 and Flag-TRAF2 alone or in combinations. Cell extracts were immunoprecipitated with anti-Flag and analyzed, after immunoblotting, with anti-Flag and anti-NEMO (upper panel). Flag-TRAF2 expression was compared with Flag-TRAF6 using an anti-Flag antiboby (lower panel).

but also by linear chains. Clearly, much remains to be done regarding this important issue. Alternatively, TRAF6 binding may play a role in anchoring NEMO in a macromolecular complex required for IKK activation. In this case, ubiquitinated TRAF6 or an associated ubiquitinated partner, such as IRAK, may attract IKK through the NUB domain and a subsequent NEMO/TRAF6 interaction occurs through the N-terminus of NEMO. Formation of such ubiquitinated multiprotein complex might play a role in recruiting the TAK complex which would eventually activate IKK through phosphorylation. Whatever the scenario involved, trying to perturb the novel interaction between the N-terminus of NEMO and TRAF6 may be exploited to dissect this sequence of event and/or to modulate IKK/NF-κB activation.

The molecular analysis of NEMO missense mutations causing IP, especially the one we report here (E57K), provide some interesting new information regarding the identity of the NF-κB-dependent signaling pathways that play a critical role in the manifestations of the disease. E57K mutation has been associated with a mild form of IP (21).

The affected female patient exhibited only dermatological defects, showing the first two stages of the disease. Because the skin lesions were not widely diffused over the body (only on the upper and lower limbs) and because no other defects were detected, this IP case was considered 'mild' and ranked as '0' using our scale of disease severity (21). In addition, she exhibited non-random but incomplete X-inactivation skewing at the time of diagnosis. Worth noting, her mother also presented mild dermatological signs, compatible with a diagnosis of familial IP.

We show here that E57K mutation is associated with a defect in TRAF6-dependent signaling pathways, such as the IL-1R and TLR pathways but not in the TNF-R1 pathway. This is, to the best of our knowledge, the first *NEMO* mutation behaving this way and this indicates that a simple impairment of this subset of signaling pathways is enough to trigger the disease, although with mild intensity. Supporting this view, mice models used to understand in more detail the pathophysiology of IP have suggested that perturbed innate immunity, which usually requires TRAF6-dependent pathways, may be the trigger of the dermatosis process, although the subsequent full-blown inflammation reaction clearly involves TNF (41). Therefore, IP patients exhibiting mutations located at the N-terminus of NEMO and affecting the TRAF6 binding site without affecting the IKK binding site may represent a class mildly affected. In contrast, patients exhibiting mutations within the NUB domain, which participates in the dual TRAF6 interaction but also binds other ubiquitinated partners, are likely to be more severely affected, such as the patient with mutation A323P (19).

Since hypomorphic mutations of *NEMO* are also responsible for EDA-ID pathology (42), EDA-ID patients, which are males, might also exist carrying mutations of the TRAF6 binding site located at the N-terminus of NEMO. Indeed, activation of IKK following pathogen exposure very often requires TRAF6 and impaired binding of TRAF6 to NEMO could cause immunodeficiency. Another main manifestation of the EDA-ID disease, anhidrotic ectodermal dysplasia, involves the ectodysplasin pathway which has been shown to utilize TRAF6 (43). Finally, the most severe cases of EDA-ID are often associated with osteopetrosis. This defect in bone remodeling is most probably caused by defective RANK signaling, which is also dependent on TRAF6 (7). Clearly, from what we have learned analyzing the molecular consequence of E57K mutation, such scenario of IP or EDA-ID association depending on the sex of the affected patient can be envisioned.

MATERIALS AND METHODS

Reagents

The following antibodies were used: anti-human NEMO (#3328, a kind gift of Dr N. Rice), anti-FLAG (Sigma-Aldrich, St Louis, MO, USA), anti-NEMO (sc-8330, Santa-Cruz, CA, USA), anti-TRAF6 (sc-7221, Santa-Cruz), anti-mouse (sc-2314, Santa-Cruz), anti-rabbit (sc-2317, Santa-Cruz). hTNF-α and hIL-1β were from Roche (Basel, Switzerland) or Peprotech (Rocky Hill, NJ, USA) and LPS from Sigma-Aldrich.
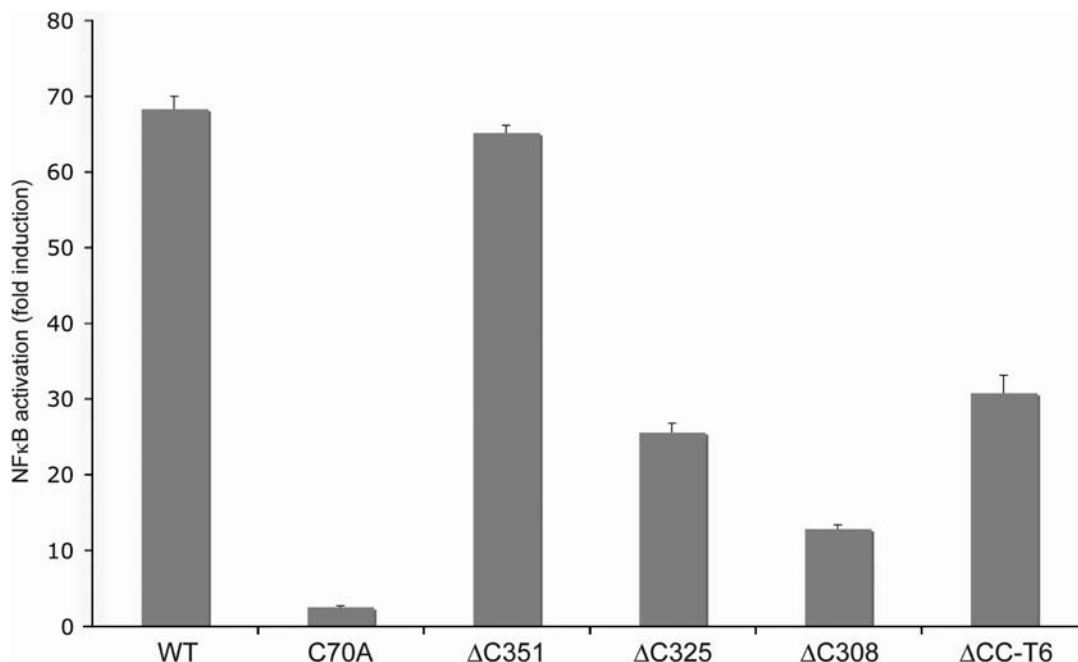
Figure 9. The coiled-coil domain of TRAF6 is involved in NF-κB activation. The various TRAF6 molecules were expressed in HEK293T and their effect on NF-κB transcriptional activity analyzed with a luciferase assay, as described in Materials and Methods. Identical expression of the proteins was confirmed after immunoblotting, using an anti-Flag antibody (data not shown).
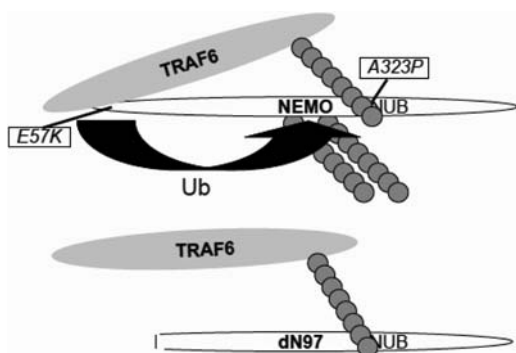

Figure 10. Dual mode of recognition between NEMO and TRAF6. Data gathered from this study and a previous one (19) indicate that NEMO directly interacts with TRAF6 through its N-terminus and recognizes ubiquitinated (Ub) TRAF6 through its NUB domain. IP-associated E57K and A323P mutations distinctly affect those two modes of interaction. Deletion ΔN97 deletion lacks the N-terminal binding site and recognizes TRAF6 through its ubiquitin moieties.

Plasmids

Mutations E57K, ΔK90, D113N, R123W and A323P of hNEMO and V316P of mNEMO have been previously described (19,21). The internal deletion in ΔCC-TRAF6 was prepared using the Quikchange mutagenesis Kit (Invitrogen, Carlsbad, CA, USA) and checked by sequencing. The truncated versions of mNEMO (ΔC385, ΔC343, ΔC299, ΔN97) were generated by PCR and inserted into pcDNA3-HA. The internal deletions of mNEMO (Δ113−168, Δ250−311, Δ201−255) were generated by enzymatic digestion and cloned into pcDNA3-HA. The deletions of hNEMO (Δ47−56, Δ57−69, Δ70−79) were a kind gift from Marienfeld

et al. (20). The truncated versions of mTRAF6 (ΔN297, ΔN319, ΔN330) were generated by PCR and inserted into pcDNA3-FLAG. Truncations ΔC325, ΔC308 and C/A were prepared using the Quickchange mutagenesis kit. The deletions of hTRAF6 (delRING=ΔN108, delTRA-FC=ΔC351) were provided by Carter and co-authors (44), the expression plasmid encoding IRAK1 by Ashwell and co-authors (45) and the pGEX-5X3-NEMO construct by Poyet (INSERM UMR 940, Hôpital Saint-Louis, Paris, France).

Cell culture and transient transfection

HEK 293T and NEMO-deficient murine embryonic fibroblasts (MEFs) (24) were cultured in Dulbecco's modified Eagle's medium (Invitrogen) supplemented with 10% fetal bovine serum, penicillin (50 U/ml) and streptomycin (50 μg/ml). Transient transfection of HEK 293T cells in six-well dishes was carried out using a standard CaPO3 procedure. Transient transfection of MEFs in 12-well dishes was performed with Lipofectamine 2000 (Invitrogen) according to the manufacturer's protocol.

Luciferase assays

For the reporter gene assays, 293T cells or MEFs were transiently transfected as described above with 200 ng of a NF-κB-dependent reporter plasmid (Igκ-Luc) and 50 ng of a renilla luciferase reporter plasmid. Equal DNA amount (2 μg/well) was maintained in each experiment by adding the appropriate empty vector to the DNA mixture. The cells were lysed after 24 h with TNT [200 mM NaCl, 1% Triton X-100, 20 mM Tris−HCl (pH 7.5)] and firefly and renilla luciferase activities

were measured according to the protocol for the dual-luciferase system (Promega, Madison, WI, USA). The resulting firefly luciferase values were normalized using the renilla values. Experiments were repeated at least three times.

Retroviral infections/stable complementation of NEMO (-) fibroblasts

PCR products derived from pcDNA3 NEMO and pcDNA3 E57K NEMO were inserted between *Bam*HI and *Eco*RI sites of pBabe-puro vector. Then, the pBabe-NEMO plasmids and empty pBabe-puro were used to transfect LinX packaging cells, using a standard CaPO3 procedure. Conditioned media collected from the transfected LinX cells after 48 h were filtered through a 0.45 µm pore size syringe filter. The viral supernatants were mixed with defined DMEM (1:1). This mixture, supplemented with polybrene (8 µg/ml, Sigma-Aldrich), was added to recipient cells, MEFs NEMO (-), that had been plated at 5×10^5 cells per 100 mm dish the day before infection. MEF cells were cultured with viral supernatants for 10 h followed by 12 h in DMEM supplemented with 10% fetal bovine serum, 100 U/ml penicillin and 100 mg/ml streptomycin. After 12 h, the cells were subjected to selection in 2 µg/ml puromycin for 14–21 days. A pool of puromycin-resistant cells was obtained and analyzed for expression of NEMO by immunoblotting.

Immunoprecipitation and western blotting

HEK 293T cells were recovered by gentle pipetting in 1 ml of PBS. They were centrifuged at 6000 rpm for 1 min in a microfuge and resuspended in 50–100 ml of TNT buffer. After incubation on ice for 10 min and centrifugation at 14 000 rpm for 10 min, the supernatant was recovered and the protein concentration determined. Proteins (100–200 mg in 200 ml of TNT) were either directly analyzed, after electrophoresis, by western blotting (see below) or immunoprecipitated. In this latter case, extracts were incubated under rotation for 2 h at 4°C with the relevant antibody. Protein A or protein G-Sepharose (Sigma) was then added and the mixture incubated for a further 1 h at 4°C. Sepharose beads were quickly centrifuged in a microfuge (30 s at 10 000 rpm) and washed three times with TNT. After the final wash, the beads were resuspended in 30 µl of buffer A [10 mM KCl, 2 mM MgCl$_2$, 0.1 mM EDTA, 1 mM DTT, 10 mM Hepes (pH 7.8)] loading dye and electrophoresed through a 10% acrylamide gel. Gels were transferred at 100 V for 1 h into Immun-Blot PVDF membranes (BioRad), which were blocked in 4% dry milk/PBS for 1 h. Incubation with the relevant Ab was carried out in 0.4% dry milk/PBS for 1 h. The membrane was washed three times in 0.05% Tween/PBS for 10 min and incubated with the secondary HPR-linked antibody for 45 min in 0.4% dry milk/PBS. After the final washes, membranes were analyzed using either ECL (Amersham, Little Chalfont, UK) or SuperSignal West Pico Chemiluminescent Kit (Pierce, Rockford, IL, USA).

GST pull-down assays

Bacteria BL21 (Invitrogen) were transformed by GST fusion plasmids (GST-hNEMO WT or GST-hNEMO A323P) and grown in LB Broth Base medium (Invitrogen) containing 100 µg/ml ampicillin and 30 µg/ml kanamycin. The expression of GST fusion proteins was induced by 1 mM IPTG for 3 h. The bacteria were collected by centrifugation, resuspended in buffer 1 (20 mM Tris–HCl (pH 7.5), 50 mM NaCl, 0.1 mM EDTA], sonicated and the lysates were centrifuged at 12 000 rpm for 10 min at 4°C. The supernatants were adjusted to 150 mM NaCl and 1% Triton X-100 and incubated with glutathione-Sepharose beads (GE Healthcare, Piscataway, NJ, USA) for 30 min at room temperature. The beads were washed three times with TEN 300 buffer [20 mM Tris–HCl (pH 7.5), 300 mM NaCl, 0.1 mM EDTA, 0.5% NP40] and conserved at 4°C, before GST pull-down assays, after verifying their quality on SDS–PAGE. Cell extracts from 293T transfected by TRAF6 were pre-cleared with gluthatione–Sepharose beads, then added to GST alone or GST-NEMO beads for 1 h at 4°C upon agitation. The beads were washed three times with lysis buffer and boiled in loading dye/SDS before analysis.

REFERENCES

1. Karin, M. and Ben-Neriah, Y. (2000) Phosphorylation meets ubiquitination: the control of NF-κB activity. *Annu. Rev. Immunol.*, **18**, 621–663.
2. Hayden, M.S. and Ghosh, S. (2008) Shared principles in NF-κB signaling. *Cell*, **132**, 344–362.
3. Scheidereit, C. (2006) IκB kinase complexes: gateways to NF-κB activation and transcription. *Oncogene*, **25**, 6685–6705.
4. Hayden, M.S. and Ghosh, S. (2004) Signaling to NF-κB. *Genes Dev.*, **18**, 2195–2224.
5. Landy, S.J. and Donnai, D. (1993) Incontinentia pigmenti (Bloch-Sulzberger syndrome). *J. Med. Genet.*, **30**, 53–59.
6. Smahi, A., Courtois, G., Vabres, P., Yamaoka, S., Heuertz, S., Munnich, A., Israël, A., Heiss, N.S., Klauck, S.M., Kioschis, P. *et al.* (2000) Genomic rearrangement in NEMO impairs NF-κB activation and is a cause of incontinentia pigmenti. *Nature*, **405**, 466–472.
7. Courtois, G. and Smahi, A. (2006) NF-κB-related genetic diseases. *Cell Death Differ.*, **13**, 843–851.
8. Nelson, D.L. (2006) NEMO, NF-κB signaling and incontinentia pigmenti. *Curr. Opin. Genet. Dev.*, **16**, 282–288.
9. Fusco, F., Pescatore, A., Bal, E., Ghoul, A., Paciolla, M., Lioi, M.B., D'Urso, M., Rabia, S.H., Bodemer, C., Bonnefont, J.P. *et al.* (2008) Alterations of the IKBKG locus and diseases: an update and a report of 13 novel mutations. *Hum. Mutat.*, **29**, 595–604.
10. Deng, L., Wang, C., Spencer, E., Yang, L., Braun, A., You, J., Slaughter, C., Pickart, C. and Chen, Z.J. (2000) Activation of the IκB kinase complex

by TRAF6 requires a dimeric ubiquitin-conjugating enzyme complex and a unique polyubiquitin chain. *Cell*, **103**, 351–361.

11. Pickart, C.M. and Eddins, M.J. (2004) Ubiquitin: structures, functions, mechanisms. *Biochim. Biophys. Acta*, **1695**, 55–72.

12. Deshaies, R.J. and Joazeiro, C.A. (2009) RING domain E3 ubiquitin ligases. *Annu. Rev. Biochem.*, **78**, 399–434.

13. Hurley, J.H., Lee, S. and Prag, G. (2006) Ubiquitin-binding domains. *Biochem. J.*, **399**, 361–372.

14. Skaug, B., Jiang, X. and Chen, Z.J. (2009) The role of ubiquitin in NF-κB regulatory pathways. *Annu. Rev. Biochem.*, **78**, 769–796.

15. Sun, S.C. (2008) Deubiquitylation and regulation of the immune response. *Nat. Rev. Immunol.*, **8**, 501–511.

16. Wertz, I.E. and Dixit, V.M. (2010) Regulation of death receptor signaling by the ubiquitin system. *Cell Death Differ.*, **17**, 14–24.

17. Yamazaki, K., Gohda, J., Kanayama, A., Miyamoto, Y., Sakurai, H., Yamamoto, M., Akira, S., Hayashi, H., Su, B. and Inoue, J. (2009) Two mechanistically and temporally distinct NF-κB activation pathways in IL-1 signaling. *Sci. Signal.*, **2**, ra66.

18. Sebban, H., Yamaoka, S. and Courtois, G. (2006) Posttranslational modifications of NEMO and its partners in NF-κB signaling. *Trends Cell. Biol.*, **16**, 569–577.

19. Sebban-Benin, H., Pescatore, A., Fusco, F., Pascuale, V., Gautheron, J., Yamaoka, S., Moncla, A., Ursini, M.V. and Courtois, G. (2007) Identification of TRAF6-dependent NEMO polyubiquitination sites through analysis of a new *NEMO* mutation causing incontinentia pigmenti. *Hum. Mol. Genet.*, **16**, 2805–2815.

20. Marienfeld, R.B., Palkowitsch, L. and Ghosh, S. (2006) Dimerization of the IκB kinase-binding domain of NEMO is required for tumor necrosis factor alpha-induced NF-κB activity. *Mol. Cell. Biol.*, **26**, 9209–9219.

21. Fusco, F., Bardaro, T., Fimiani, G., Mercadante, V., Miano, M.G., Falco, G., Israël, A., Courtois, G., D'Urso, M. and Ursini, M.V. (2004) Molecular analysis of the genetic defect in a large cohort of IP patients and identification of novel NEMO mutations interfering with NF-κB activation. *Hum. Mol. Genet.*, **13**, 1763–1773.

22. Rushe, M., Silvian, L., Bixler, S., Chen, L.L., Cheung, A., Bowes, S., Cuervo, H., Berkowitz, S., Zheng, T., Guckian, K. *et al.* (2008) Structure of a NEMO/IKK-associating domain reveals architecture of the interaction site. *Structure*, **16**, 798–808.

23. Courtois, G., Whiteside, S.T., Sibley, C.H. and Israël, A. (1997) Characterization of a mutant cell line that does not activate NF-κB in response to multiple stimuli. *Mol. Cell Biol.*, **17**, 1441–1449.

24. Schmidt-Supprian, M., Bloch, W., Courtois, G., Addicks, K., Israël, A., Rajewsky, K. and Pasparakis, M. (2000) NEMO/IKKγ-deficient mice model incontinentia pigmenti. *Mol. Cell*, **5**, 981–992.

25. Lo, Y.C., Lin, S.Y., Rospigliosi, C.C., Conze, D.B., Wu, C.J., Ashwell, J.D., Eliezer, D. and Wu, H. (2009) Structural basis for recognition of diubiquitins by NEMO. *Mol. Cell.*, **33**, 602–615.

26. Grubisha, O., Kaminska, M., Duquerroy, S., Fontan, E., Cordier, F., Haouz, A., Raynal, B., Chiaravalli, J., Delepierre, M., Israël, A. *et al.* (2010) DARPin-assisted crystallography of the CC2-LZ domain of NEMO reveals a coupling between dimerization and ubiquitin binding. *J. Mol. Biol.*, **395**, 89–104.

27. Kovalenko, A., Chable-Bessia, C., Cantarella, G., Israël, A., Wallach, D. and Courtois, G. (2003) The tumour suppressor CYLD negatively regulates NF-κB signalling by deubiquitination. *Nature*, **424**, 801–805.

28. Kanayama, A., Seth, R.B., Sun, L., Ea, C.K., Hong, M., Shaito, A., Chiu, Y.H., Deng, L. and Chen, Z.J. (2004) TAB2 and TAB3 activate the NF-κB pathway through binding to polyubiquitin chains. *Mol. Cell.*, **15**, 535–548.

29. Walsh, M.C., Kim, G.K., Maurizio, P.L., Molnar, E.E. and Choi, Y. (2008) TRAF6 autoubiquitination-independent activation of the NF-κB and MAPK pathways in response to IL-1 and RANKL. *PLoS ONE*, **3**, e4064.

30. Lamothe, B., Campos, A.D., Webster, W.K., Gopinathan, A., Hur, L. and Darnay, B.G. (2008) The RING domain and first zinc finger of TRAF6 coordinate signaling by interleukin-1, lipopolysaccharide, and RANKL. *J. Biol. Chem.*, **283**, 24871–24880.

31. Conze, D.B., Wu, C.J., Thomas, J.A., Landstrom, A. and Ashwell, J.D. (2008) Lys63-linked polyubiquitination of IRAK-1 is required for interleukin-1 receptor- and toll-like receptor-mediated NF-κB activation. *Mol. Cell Biol.*, **28**, 3538–3547.

32. Windheim, M., Stafford, M., Peggie, M. and Cohen, P. (2008) Interleukin-1 (IL-1) induces the Lys63-linked polyubiquitination of IL-1 receptor-associated kinase 1 to facilitate NEMO binding and the activation of IκBα kinase. *Mol. Cell. Biol.*, **28**, 1783–1791.

33. Sun, L., Deng, L., Ea, C.K., Xia, Z.P. and Chen, Z.J. (2004) The TRAF6 ubiquitin ligase and TAK1 kinase mediate IKK activation by BCL10 and MALT1 in T lymphocytes. *Mol. Cell.*, **14**, 289–301.

34. tokunaga, F., Sakata, S., Saeki, Y., Satomi, Y., Kirisako, T., Kamei, K., Nakagawa, T., Kato, M., Murata, S., Yamaoka, S. *et al.* (2009) Involvement of linear polyubiquitylation of NEMO in NF-κB activation. *Nat. Cell. Biol.*, **11**, 123–132.

35. Leonardi, A., Chariot, A., Claudio, E., Cunningham, K. and Siebenlist, U. (2000) CIKS, a connection to IκB kinase and stress-activated protein kinase. *Proc. Natl Acad. Sci. USA*, **97**, 10494–10499.

36. Wu, Z.H., Shi, Y., Tibbetts, R.S. and Miyamoto, S. (2006) Molecular linkage between the kinase ATM and NF-κB signaling in response to genotoxic stimuli. *Science*, **311**, 1141–1146.

37. Mabb, A.M., Wuerzberger-Davis, S.M. and Miyamoto, S. (2006) PIASy mediates NEMO sumoylation and NF-κB activation in response to genotoxic stress. *Nat. Cell. Biol.*, **8**, 986–993.

38. Napolitano, G., Mirra, S., Monfregola, J., Lavorgna, A., Leonardi, A. and Ursini, M.V. (2009) NESCA: a new NEMO/IKKgamma and TRAF6 interacting protein. *J. Cell. Physiol.*, **220**, 410–417.

39. Yang, K., Zhu, J., Sun, S., Tang, Y., Zhang, B., Diao, L. and Wang, C. (2004) The coiled-coil domain of TRAF6 is essential for its auto-ubiquitination. *Biochem. Biophys. Res. Commun.*, **324**, 432–439.

40. Yin, Q., Lin, S.C., Lamothe, B., Lu, M., Lo, Y.C., Hura, G., Zheng, L., Rich, R.L., Campos, A.D., Myszka, D.G. *et al.* (2009) E2 interaction and dimerization in the crystal structure of TRAF6. *Nat. Struct. Mol. Biol.*, **16**, 658–666.

41. Nenci, A., Huth, M., Funteh, A., Schmidt-Supprian, M., Bloch, W., Metzger, D., Chambon, P., Rajewsky, K., Krieg, T., Haase, I. *et al.* (2006) Skin lesion development in a mouse model of incontinentia pigmenti is triggered by NEMO deficiency in epidermal keratinocytes and requires TNF signaling. *Hum. Mol. Genet.*, **15**, 531–542.

42. Döffinger, R., Smahi, A., Bessia, C., Geissmann, F., Feinberg, J., Durandy, A., Bodemer, C., Kenwrick, S., Dupuis-Girod, S., Blanche, S. *et al.* (2001) X-linked anhidrotic ectodermal dysplasia with immunodeficiency is caused by impaired NF-κB signaling. *Nat. Genet.*, **27**, 277–285.

43. Naito, A., Yoshida, H., Nishioka, E., Satoh, M., Azuma, S., Yamamoto, T., Nishikawa, S. and Inoue, J. (2002) TRAF6-deficient mice display hypohidrotic ectodermal dysplasia. *Proc. Natl Acad. Sci. USA*, **99**, 8766–8771.

44. Gentry, J.J., Rutkoski, N.J., Burke, T.L. and Carter, B.D. (2004) A functional interaction between the p75 neurotrophin receptor interacting factors, TRAF6 and NRIF. *J. Biol. Chem.*, **279**, 16646–16656.

45. Conze, D.B., Wu, C.J., Thomas, J.A., Landstrom, A. and Ashwell, J.D. (2008) Lys63-linked polyubiquitination of IRAK-1 is required for interleukin-1 receptor- and toll-like receptor-mediated NF-κB activation. *Mol Cell Biol.*, **28**, 3538–3547.